Calcaneal Fixation Plate Test Method Development

Dana J. Coombs, Sherri Wykosky, and Michael Bushelow

DePuy Synthes Trauma

Abstract: *Standard ASTM test methods, such as four point bend tests based on ASTM F382, do not apply well to fixation plates with complex geometry and loading. The objective of this study was to develop a test method, using typical mechanical testing equipment, which would match the musculoskeletal loads on the calcaneus bone during gait.*

This study used the AnyBody Modeling System Foot Model to determine muscle, ligament, and joint contact forces during gait. Abaqus input files were created which contained all loads in the model as a function of gait. ScanIP was used to process the tessellated calcaneus, model a Sanders IIb fracture pattern, and generate an Abaqus mesh. The DePuy Synthes 3.5mm Locking Calcaneal Plate and corresponding screws were assembled to the calcaneus in Abaqus/CAE. The model was run using the Abaqus/Standard implicit solver.

The greatest stresses in the plate occurred at "toe off" during the stance phase of gait. Free Body Cuts determined the internal loads and moments along the plate length. Simplified shear and moment diagrams were created to determine a 3 point bend test configuration. Free body diagrams were used to determine support locations and direction of applied loads.

A second finite element model was developed, using Abaqus/CAE, to simulate the test configuration.

Qualitatively, the maximum principal stress distribution matched well between the musculoskeletal and test method models. A three point bend test method, which includes offset loading to create out of plane bending, can be used to replicate the musculoskeletal loads.

Keywords*: Calcaneal, Calcaneus, Ankle, Foot, Biomechanics, Computational Biomechanics, Musculoskeletal, Gait, Internal Fixation, Trauma, Orthopedic, Free Body Cuts, Free Body Diagrams, Test, Test Method, ASTM, Fatigue*

1. Introduction

Standard ASTM test methods, such as four point bend tests based on ASTM F382, do not apply well to internal fixation trauma plates with complex geometry and loading conditions such as plates for repair of the calcaneus. The objective of this study was to develop a test method that would evaluate these types of plates under more realistic/physiologic loading conditions. To develop the test method, this study used a detailed musculoskeletal model of the foot to determine muscle, ligament, and joint contact forces during gait, and finite element techniques to develop a better test method. A Sanders IIb fracture pattern was used for this study.

2. Materials and Methods

The internal fixation trauma plate used for this study was the DePuy Synthes 3.5mm Locking Calcaneal Plate (241.622, Revision C) and 3.5mm, self-tapping, Locking Stardrive screws.

2.1 Musculoskeletal Loads

The AnyBody Modeling System™ (AnyBody Technology, Aalborg, Denmark) was used to estimate the loads applied on the calcaneous bone during the stance phase of a healthy person walking. The foot model is integrated with a leg model to ensure realistic muscle forces, as several leg muscles span the ankle. This system uses inverse dynamics.

The AnyBody foot model contains all the individual foot bones, all the intrinsic foot muscles and the major ligaments. It was developed using data from literature about joints' type, position and orientation, as well as muscles and ligaments' attachment points and mechanical properties. The entire foot model is shown in Figure 1.

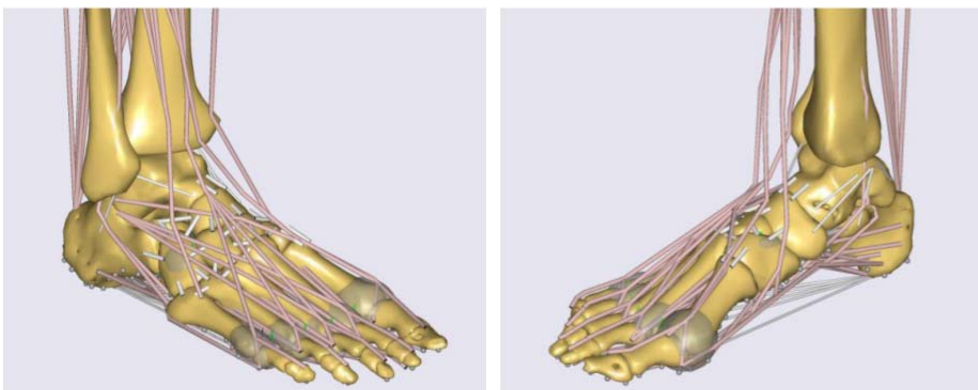

Figure 1: AnyBody Technology Foot Model

The calcaneus bone receives loads from various mechanical structures:

- Two joints; subtalar joint and calcaneo-cuboid joint. Both joints are created as revolute joints. The joints can be seen in Figure 2.
- Muscles: Attached directly to the bone: (Gastrocnemius, Soleus, plantaris, Extensor Hallucis Brevis, Extensor Digitorum Brevis, Quadratus Plantar, Abductor Hallucis, Flexor Digitorum Brevis, Abductor Digiti Minimi). Through via points, sliding on the surface or in ligamentous tunnels: (Peroneus Longus, Peroneus Brevis, Tibialis Posterior, Flexor Digitorum Longus, Flexor Hallucis Longus). The muscles are shown in Figure 3.
- Ligaments: Tibiocalcaneal, Calcaneofibular, Calcaneonavicular, Calcaneocuboid Plantar and Dorsal, Bifurcate, Long Plantar and Plantar Aponeurosis. The ligaments can be seen in Figure 4.

- Floor: The reaction force was measured with a force plate and a pressure sensitive plate to measure the plantar pressure distribution and applied to the bone. The pressure distribution can be seen in Figure 5.

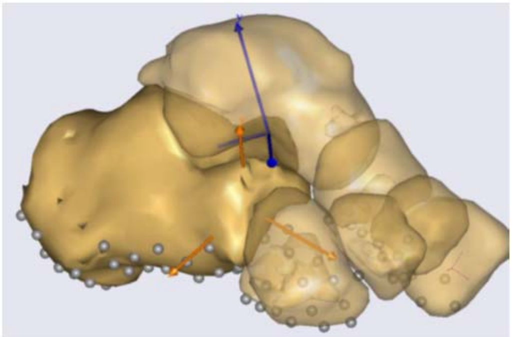

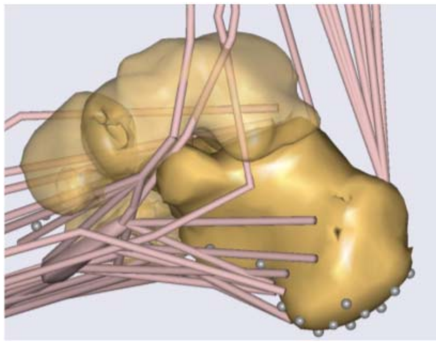

Figure 2: Subtalar / Calcaneo-Cuboid Joint **Figure 3: Muscles**

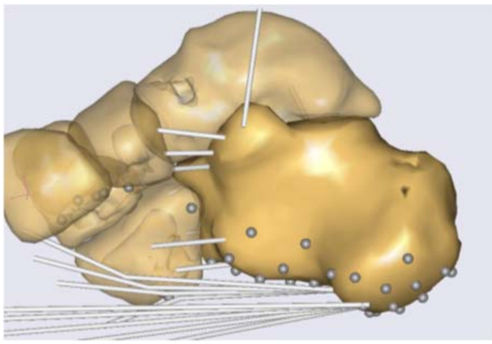

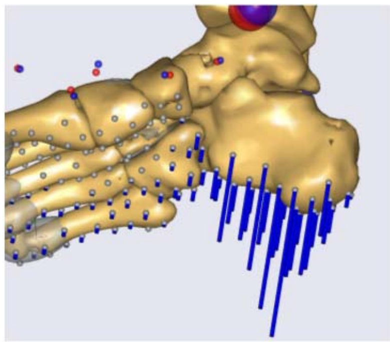

Figure 4: Ligaments **Figure 5: Ground Reaction**

The loads on the calcaneus bone were computed for the stance phase of walking based on a subject weighing 76 kg with a foot length of 0.235 m. Motion capture data was imposed on the model and ground reaction force was recorded simultaneously by a force plate and a pressure plate. By mapping the pressure map on the foot surface, it was possible to apply the correct share of the ground reaction force to each individual bone. A series of force vectors were then applied to a grid on the surface of each bone according to the recorded pressure distribution. Figure 6 shows snap shots of the inverse dynamic analysis of the stance phase of walking. Activated muscles are visible (bulged and dark colored), as well as the applied pressure load (thin blue lines).

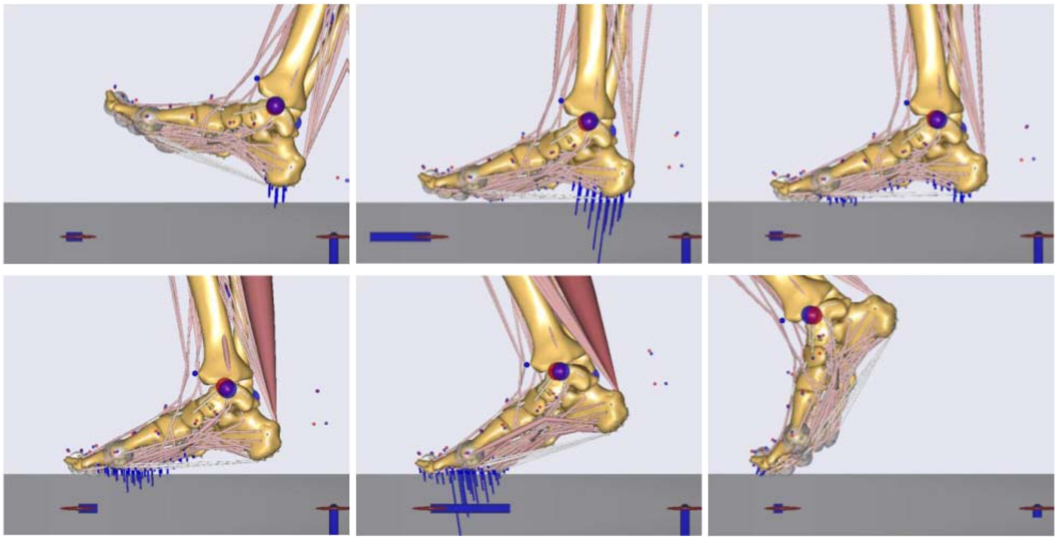

Figure 6: Frames of Stance Phase of Gait

The analysis time, which was the time of stance during gait, was 0.727 to 1.295 seconds. The output of this analysis was Abaqus input files, which contained all loads in the model. The loads were defined as amplitudes that vary over time and used a coupling constraint to connect the load point of application to the mesh of the bone. In addition, the tessellated (.stl) file of the subject's calcaneus bone was provided.

2.2 Defining Bone Geometry, Fracture, and Mesh

ScanIP (simpleware, Exeter, UK) was used to process the tessellated (.stl) file for the subject used in the musculoskeletal model and generate a finite element mesh. The original tessellated file only included the cortical shell, which included holes in the shell. The tessellated file was opened in the +CAD application and converted to a mask. During mask conversion, resampling with smooth artifacts option was used to remove the holes and smooth the outside surface. The file was saved as a ScanIP file. The file was opened in ScanIP and a flood fill segmentation tool was used to fill in the internal void of the mask.

The fractures were modeled in ScanIP using primitive cuboids and mask cuts. The fractures approximated the location of fracture lines of a Sanders IIb fracture, as estimated by Illert et al. The final fractured bone model can be seen in Figure 7 along with a photograph of the fracture used by Illert et al. for comparison purposes. An Abaqus mesh of the calcaneus was generated using the +FE Free mesh algorithm with a node set defined for the external surface of the mesh and C3D4 linear tetrahedral elements. The external surface node set was used to constrain the loads to the mesh.

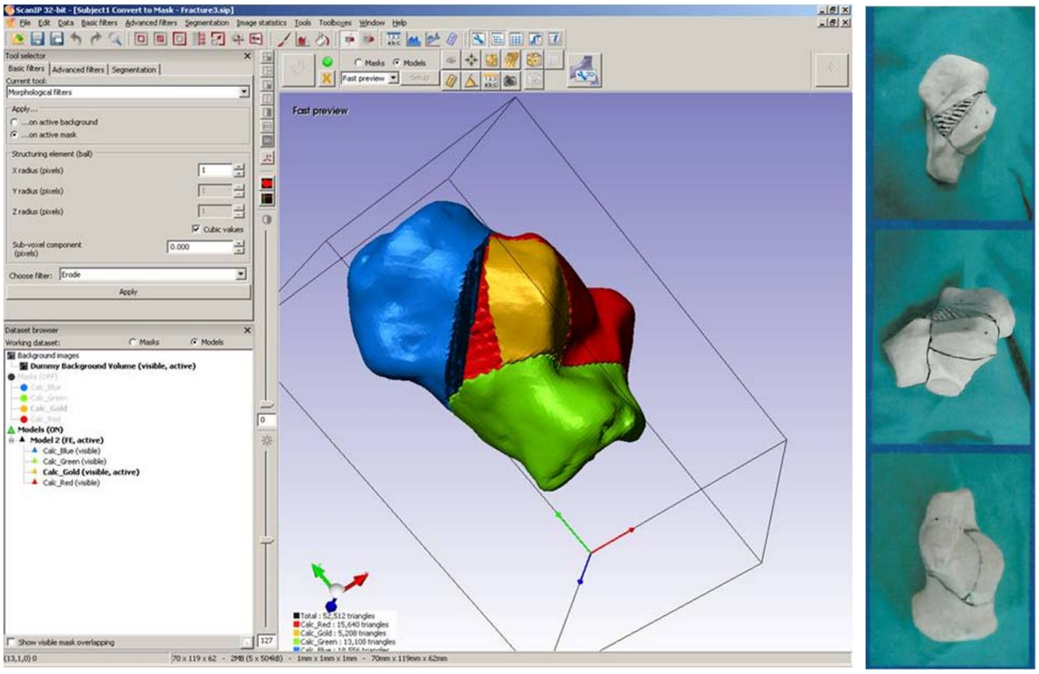

Figure 7: Sanders IIb Fracture

2.3 Defining the Musculoskeletal Finite Element Model

The fractured calcaneus mesh input file and the AnyBody Technology input file, representing the applied loads, were imported into Abaqus/CAE. As mentioned in Section 2.2, the elements in the bone mesh were C3D4 linear tetrahedral elements. A coupling constraint was used to connect the load point of application to the external node set on the mesh of the bone. The 3.5mm Locking Calcaneal Plate was assembled to the calcaneus. The plate and screws were meshed with C3D10 quadratic tetrahedral elements. The mesh density was defined such that a minimum of 2 elements were defined across the thickness of the plate. Each screw body was constrained to the mesh of the bone using a tie constraint between the screw surface and the nodes in the bone mesh. The screw heads were constrained to the plate using a tie constraint between the surfaces of the screw heads and the plate holes. Figure 8 shows the forces and the constraints in the model. The plates and screws were defined as stainless steel ($E = 186400$ MPa, $\nu = 0.3$). The bone used a less stiff material property, but stiff enough to transfer loads to the plate and not deform grossly ($E=20000$ MPa, $\nu = 0.3$). The model was run with the Abaqus/Standard implicit solver using the loads which varied over time as defined in section 2.1.

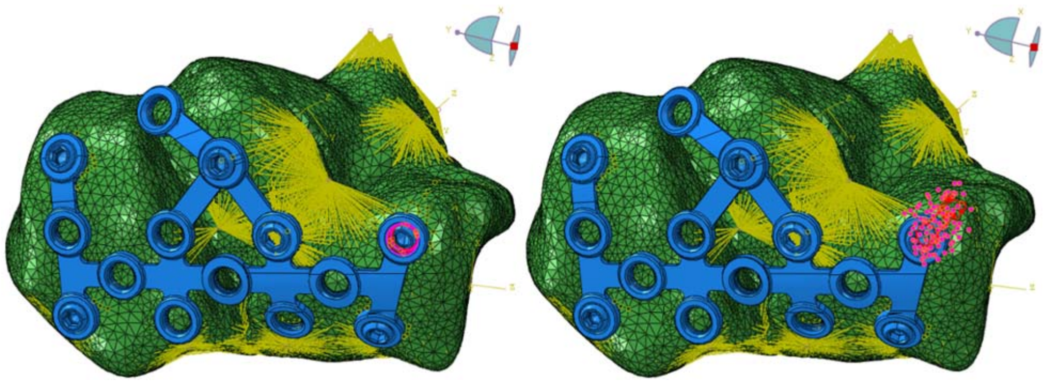

Figure 8: Musculoskeletal Model - Forces and Constraints

The result of the analysis was used to determine the greatest stresses in the plate during the stance phase of gait, based on maximum principal stress. Figure 9 shows the maximum principal stress distribution at the worst case frame during the stance phase, which was 1.191 seconds. The internal loads and moments in the plate were determined every 3mm along the length of the plate using Free Body Cuts in Abaqus/CAE. Figure 10 shows an example of one Free Body Cut and the relative coordinate system used to define the cuts normal to the Y axis. The orientation was consistent as the Free Body Cut moved along the plate in the Y direction.

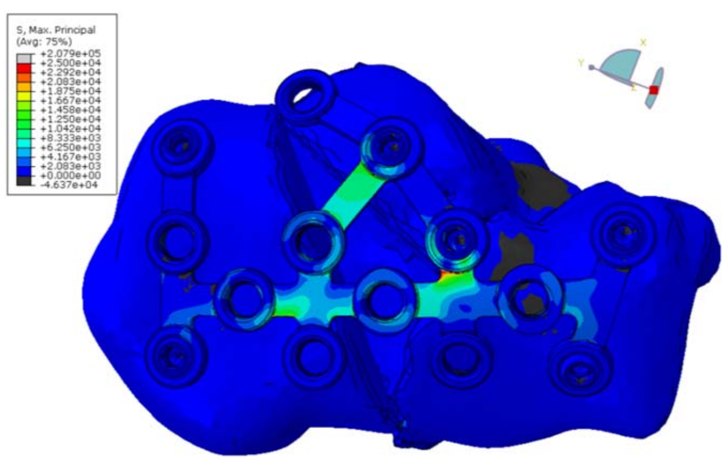

Figure 9: Worst Case Frame

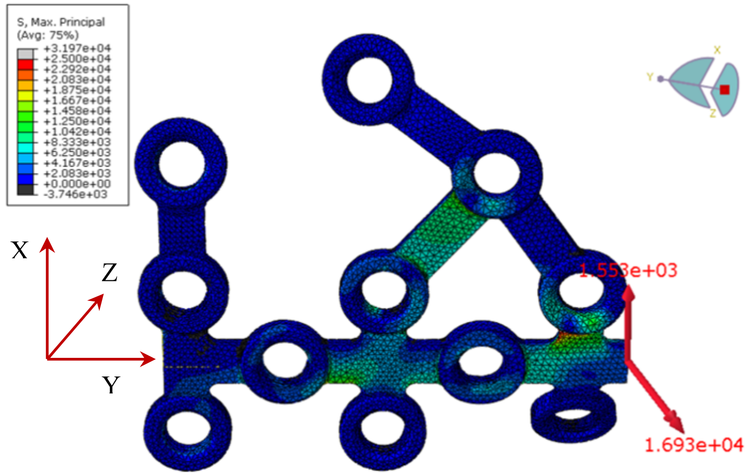

Figure 10: Free Body Cut

2.4 Determining Internal Loads

The internal loads and moments in the plate, based on the Free Body Cuts at frame 1.191 seconds, were graphed along the length of the plate in the Y direction. Figure 11 shows the graphs of the internal forces and moments. Erratic behavior is seen near the tie constraints between the screw heads and the plate, which can generate high stress and singularities in the results.

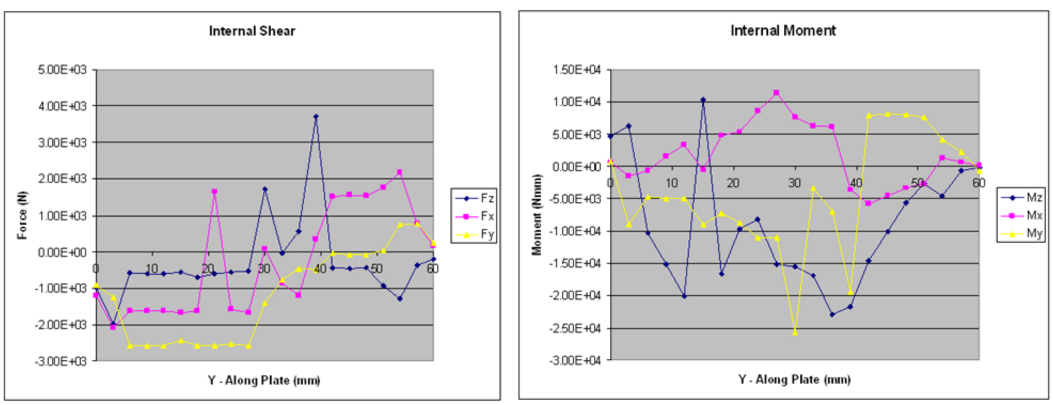

Figure 11: Internal Shear and Moment along Y

Upon examining the data, it seemed possible to reproduce these internal forces and moments by using a 3 point bend configuration in the X-Y plane (ignoring the results near the tie constraints). Figure 12 shows a graph of the internal force and moment with an assumed, qualitative 3 point bend shear and moment result. Generally, the X direction shear loads have a step and moments about the Z axis have a linear increase and decrease. The X direction shear load step and the moments about the Z axis inflection occur at the same location, which matches a shear and moment diagram for a 3 point bend configuration.

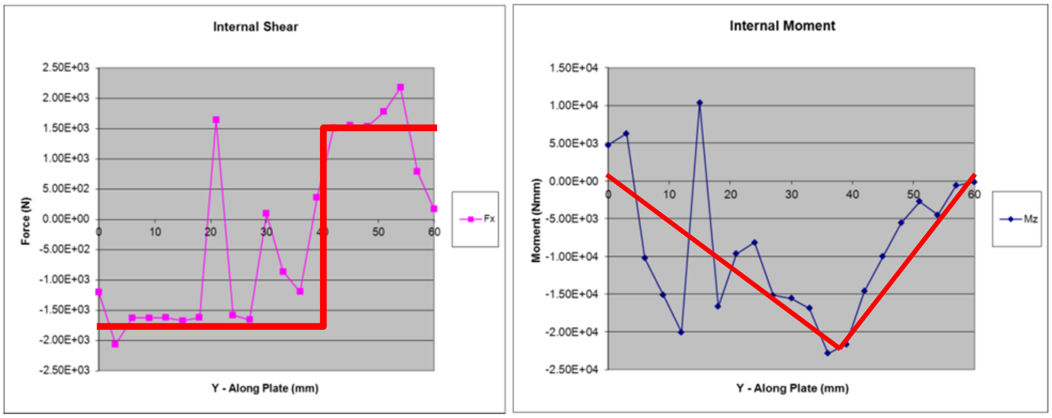

Figure 12: Overlay of 3 Point Bend Shear and Moment Diagram

2.5 Determining a 3 Point Bend Configuration

To determine a 3 point bend test configuration, the internal Free Body Cuts were used to create free body diagrams to determine the location of supports and direction of applied loads. The initial assumption was that this is a planar problem and the left and right side support was a simple pin support.

2.5.1 Free Body Diagram 1

The first free body diagram used the left side of the plate at 12mm from the left edge along the Y-Axis, and is referred to as FBD 1. The 12mm location was away from screws and was in the constant value area of the X direction shear load. The free body diagram includes the X direction shear load, Z direction moment, and the X-Y loads applied to a support pin on the left side of the plate. There are 3 equations for planar static equilibrium:

- Summation of forces in X direction
- Summation of forces in Y direction
- Summation of moments about Z direction

There were 4 unknowns:

- Support location in X direction (Rx1)
- Support location in Y direction (Ry1)
- Support reaction force in X direction (Fx1)
- Support reaction force in Y direction (Fy1)

The support location in the Y direction was assumed to be -25mm, relative to the coordinate system. This reduces the unknown parameters to 3, which can be solved with the 3 equations of static equilibrium. Figure 13 shows the free body diagram, equations of static equilibrium, and the solution to the unknown parameters.

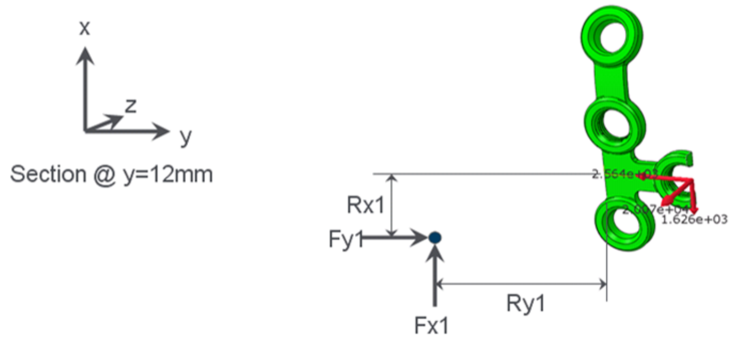

(1) $\sum F_x = 0: \ -1626 + F_{x1} = 0$

(2) $\sum F_y = 0: \quad 2564 + F_{y1} = 0$

(3) $\sum M_{z\ (@y=0)} = 0: \quad -20070 + F_{x1}R_{y1} + F_{y1}R_{x1} + 1626(12) = 0$

Assume $R_{y1} = -25mm, solve$:

$F_{x1} = 1626N$

$F_{y1} = 2564N$

$R_{x1} = -15.64mm$

Figure 13: Free Body Diagram 1

2.5.2 Free Body Diagram 2

The second free body diagram used the right side of the plate at 42mm from the left edge of the plate along the Y-Axis, and is referred to as FBD 2. The 42mm location was away from screws and was in the constant value area of the X direction shear load. The free body diagram includes the X direction shear load, Z direction moment, and the X-Y loads applied to a support pin on the right side of the plate. The same 3 equations for planar static equilibrium were used.

There were 4 unknowns:

- Support location in X direction (Rx2)
- Support location in Y direction (Ry2)
- Support reaction force in X direction (Fx2)
- Support reaction force in Y direction (Fy2)

The support location in the Y direction was assumed to be 60mm, relative to the coordinate system. This reduces the unknown parameters to 3, which can be solved with the 3 equations of static equilibrium. Figure 14 shows the free body diagram, equations of static equilibrium, and the solution to the unknown parameters.

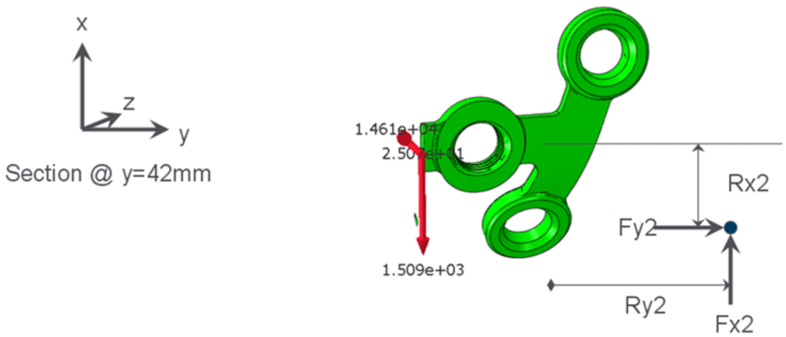

(4) $\sum F_x = 0: \quad -1509 + F_{x2} = 0$

(5) $\sum F_y = 0: \quad 25.07 + F_{y2} = 0$

(6) $\sum M_{z\,(@y=0)} = 0: \quad 14610 - F_{x2}R_{y2} + F_{y2}R_{x2} + 1509(42) = 0$

Assume $R_{y2} = 60mm, solve$:

$F_{x2} = 1509N$

$F_{y2} = -25.07N$

$R_{x2} = 500.68mm$

Figure 14: Free Body Diagram 2

2.5.3 Free Body Diagram 3

The third free body diagram used the entire plate and is referred to as FBD 3. The free body diagram includes the reaction loads at the support locations in the X and Y direction and the input load in the middle of the plate. The input load has both the X and Y components. The same 3 equations for planar static equilibrium were used.

There were 4 unknowns:

- Support location in X direction (Rx3)
- Support location in Y direction (Ry3)
- Support reaction force in X direction (Fx3)
- Support reaction force in Y direction (Fy3)

The input load location in the Y direction was assumed to be 15mm, relative to the coordinate system. This reduces the unknown parameters to 3, which can be solved with the 3 equations of static equilibrium. Figure 15 shows the free body diagram, equations of static equilibrium, and the solution to the unknown parameters.

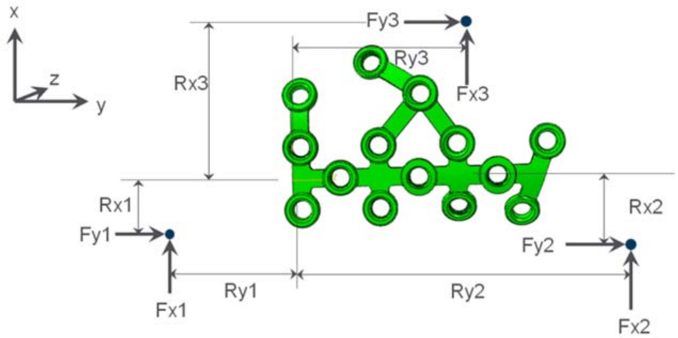

(7) $\sum F_x = 0$: $F_{x1} + F_{x2} + F_{x3} = 0$

(8) $\sum F_y = 0$: $F_{y1} + F_{y2} + F_{y3} = 0$

(9) $\sum M_{z\,(@y=0)} = 0$: $-F_{x1}R_{y1} + F_{y1}R_{x1} - F_{x2}R_{y2} + F_{y2}R_{x2} - F_{x3}R_{y3} + F_{y3}R_{x3} = 0$

Assume $R_{y3} = 15mm, solve$:

$F_{x3} = -3135N$

$F_{y3} = -2538.93N$

$R_{x2} = -21.86mm$

Figure 15: Free Body Diagram 3

2.5.4 Free Body Diagram Summary

Figure 16 shows a summary of the load locations and the load values. The image also shows the vector directions, represented as red, dashed lines. Based on static equilibrium, the load vectors can be applied anywhere along the vector lines.

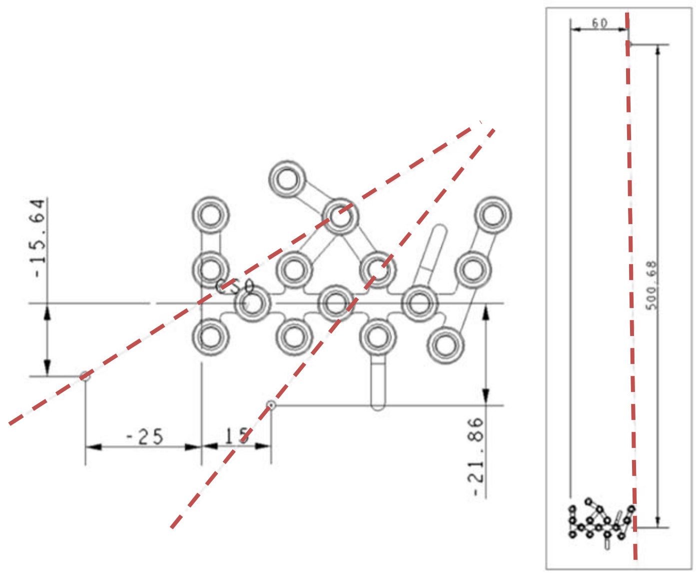

Figure 16: Free Body Diagram Summary

2.6 Defining and Simulating the Test Method

A physical test method was designed based on the free body diagram results. The test blocks were designed such that the roller supports and point of load application were along the vector lines defined in section 2.5.4. Rather than using a pin support on the right side of the model, a roller support was used and the surface of the test block was normal to the vector line. The roller support was brought closer to the plate so that the test construct was feasible to fit and run on a standard test frame. The test setup was modeled in Pro/ENGINEER and imported into Abaqus/CAE. The same material models, mesh density, and interactions between the screw head and plate were used. The test blocks material models were defined as Objet VeroWhite (E = 2500 MPa), which is used by the Objet 3D printer. The screw body was constrained to the holes in the test blocks using a tie constraint between the screw surfaces and the hole surfaces in the test blocks. The screw head was constrained to the plate using a tie constraint between the surfaces of the screw head and the plate hole. A reference point was created at the center of the left pin hole and connected to the hole surface using a tie kinematic coupling constraint. The constraints removed all degrees of freedom except rotation about Z, to replicate a pin. A second reference point was created on the bottom surface of the right test block along the line contact of the right support roller. This reference point was connected to the bottom surface of the right test block using a kinematic coupling. This point was constrained such that the roller was allowed to slide along the bottom surface, but only rotate about the axis of the roller. A third reference point was created at the center of the concave spherical cut, which is where a ball would apply load through the actuator. This reference point was connected to the spherical cut using a kinematic coupling.

The original model had a Z location for the actuator reference point at -2.39mm, which was consistent with the out of plane moment measured inside the plate. The stress distribution matched well with the exception of the top triangular strut. To increase the stress in that area, the Z direction of the reference point was moved further away from the plate. The Z value of -31.2mm was a good qualitative match to the results. Figure 17 shows the test setup.

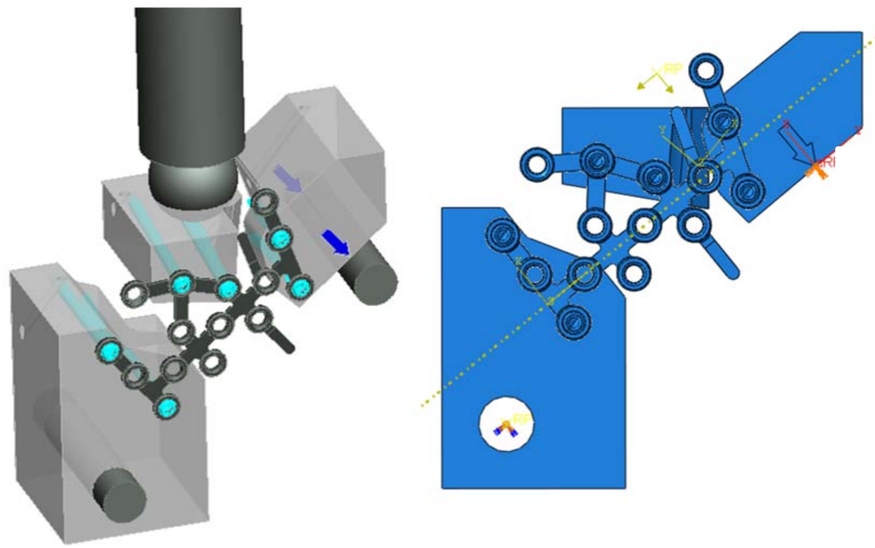

Figure 17: Test Setup

3. Results

Figure 18 shows the results of the calcaneus musculoskeletal model and test method model. Qualitatively, the maximum principal stress distribution matched well. However, the stresses in the test method model are lower. Two main factors could explain this result. First, the plate was modeled as planar and not bent to fit the calcaneus. Second, the boundary conditions are not exactly the same because the right support pin does not match the boundary conditions of the point free body diagram model. However, these boundary conditions were determined based on a feasible test setup. The most important result was to match the stress distribution, not the actual stress values.

The stress results exceed the yield strength of the stainless steel material. It is not assumed that someone would apply normal gait loads with a fractured calcaneus even with fixation. The goal of this study was to determine the load and support locations and vectors. The magnitudes will be much lower during actual testing. In addition, contact was not modeled between the fractured bone segments. This creates a worst case stress situation since all the load must transfer through the plate.

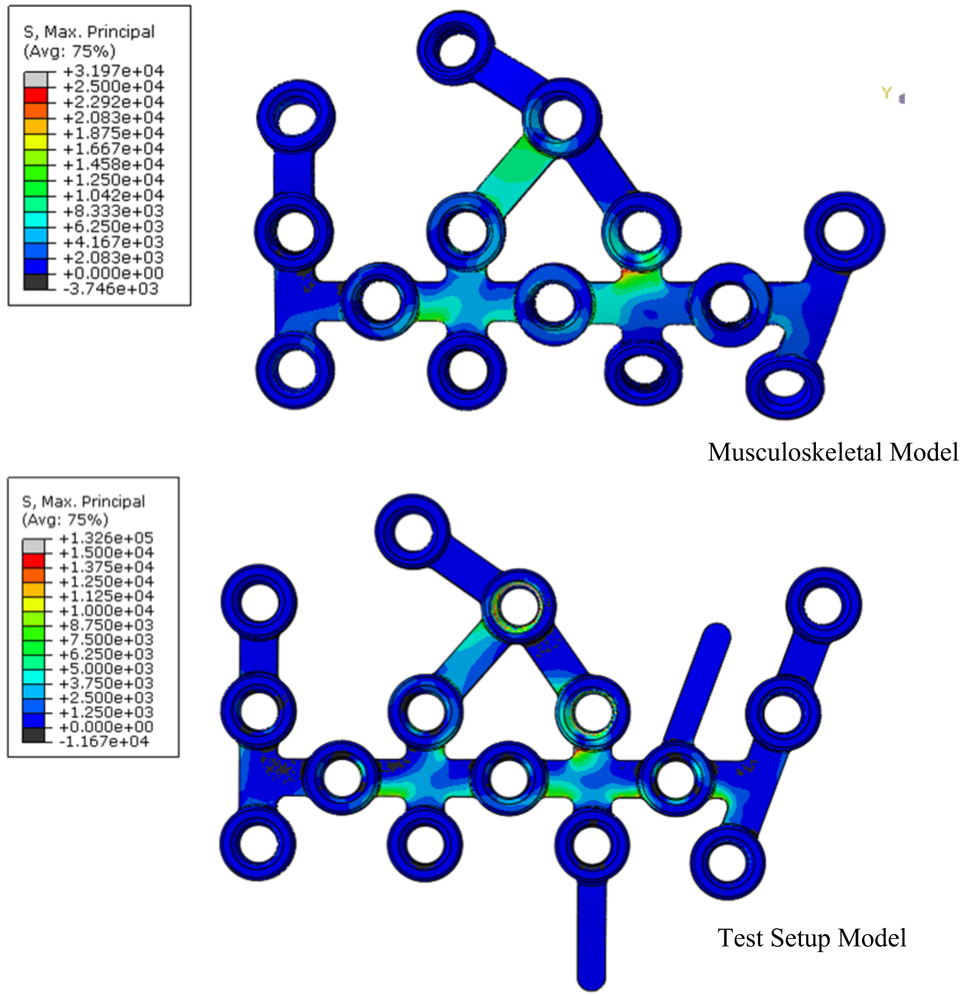

Figure 18: Stress Distribution Comparison

Physical fatigue mechanical testing was performed on the 3.5mm Locking Calcaneal Plate with this test setup. The failure location matched the area of highest maximum principal stress as shown in Figure 19.

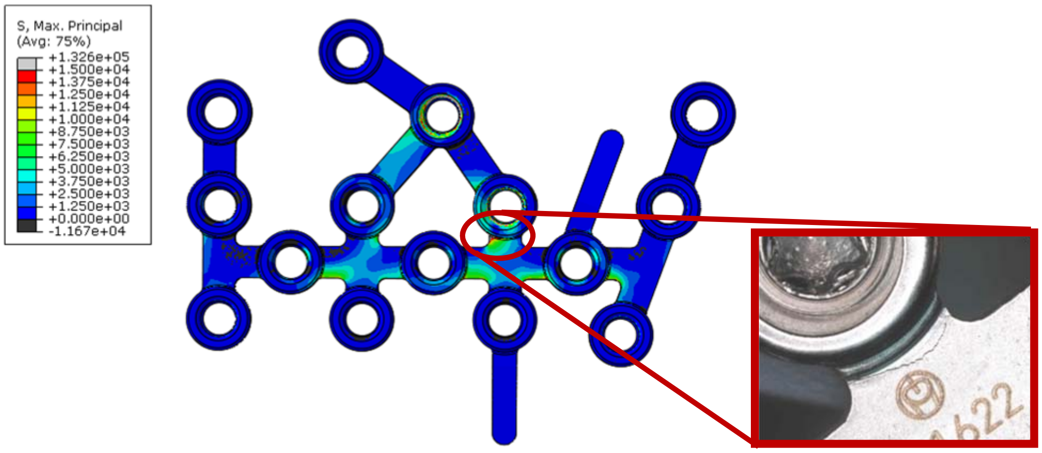

Figure 19: Fatigue Failure Correlation

4. Conclusions

A three point bend test setup with a pin roller, a sliding roller, and a point load of application represents a similar loading condition to the worst case frame of a gait cycle. In addition, the mechanical testing failure mode was predicted by the simulation of the test setup.

Finite element models are powerful to determine the performance of an orthopedic device and determine test methods. Future study could also be pursued to simulate the development of mesh-independent fractures of the bone with X-FEM, which would also account for the contact between bone segments.

5. References

1. Illert T., Rammelt S, Drewes T., Grass R., Zwipp, H., "Stability of locking and non-locking plates in an osteoporotic calcaneal fracture model," Foot & Ankle International., 32 (3-March): 307-313, 2011